Shape and electromagnetic properties of the ^{229m}Th isomer

Nikolay Minkov[1,2,*] and *Adriana* Pálffy[2,3]

[1]Institute of Nuclear Research and Nuclear Energy, Bulgarian Academy of Sciences, Tzarigrad Road 72, BG-1784 Sofia, Bulgaria
[2]Max-Planck-Institut für Kernphysik, Saupfercheckweg 1, D-69117 Heidelberg, Germany
[3]Department of Physics, Friedrich-Alexander-Universität Erlangen-Nürnberg, D-91058 Erlangen, Germany

Abstract. We examine the physical conditions, and specifically the role of the quadrupole-octupole deformation, for the emergence of the 8 eV "clock" isomer ^{229m}Th. Our nuclear structure model suggests that such an extremely low-energy state can be the result of a very fine interplay between the shape and single-particle (s.p.) dynamics in the nucleus. We find that the isomer can only appear in a rather limited region of quadrupole-octupole deformation space close to a line along which the ground-state and isomer s.p. orbitals 5/2[633] and 3/2[631], respectively, cross each other providing the isomer-formation quasi-degeneracy condition. The crucial role of the octupole deformation in the formation mechanism is pointed out. Our calculations within the outlined deformation region show a smooth behaviour of the ^{229}Th electromagnetic properties, including the isomer decay rate, allowing for their more precise theoretical determination.

1 Introduction

The ^{229m}Th nuclear isomer attracts much interest related to its exceptionally low energy of approximately 8 eV which appears to be accessible for the contemporary vacuum ultraviolet (VUV) lasers [1] and thus opens the possibility for a number of valuable applications such as the establishing of a new frequency standard, "nuclear clock" [2–4], development of nuclear lasers in the optical range [5] and others [6, 7]. The achieving of these goals, however, requires very precise knowledge of the isomer energy, life-time and the related nuclear electromagnetic characteristics. Following this motivation several recent experimental studies have been focused on the isomer decay modes and provided estimates about its life time in charged [8] and neutral [9] electronic states. Further, the magnetic dipole moment μ in the isomeric state (IS) was determined for the first time in laser spectroscopy experiments providing the value of $\mu_{\rm IS} = -0.37(6)\mu_N$ [10, 11]. Then, three very recent experiments provided newly updated values for the isomer energy, $E_{IS} = 8.28(17)$ eV [12] from internal conversion electron spectroscopy, $E_{IS} = 8.30(92)$ eV [13] by determining the transition rates and energies from the above level at 29.2 keV and $E_{IS} = 8.10(17)$ eV [14] from a micro-calorimetric determination of absolute γ-ray energy differences.

Yet the direct nuclear decay transition of the ^{229m}Th isomer is not observed experimentally. This imposes the need of detailed theoretical examination and prediction of its nuclear electromagnetic characteristics. The problem is additionally complicated due to the rich deformation properties of the actinide nuclei to which the nucleus ^{229}Th belongs. Trying to address the above aspects recently we initiated a theoretical study [15], exploring a nuclear model approach which incorporates the shape-dynamic properties together with the intrinsic structure characteristics typical for the actinide region where the quadrupole-octupole (QO) deformation manifests. The formalism includes a description of the collective QO vibration-rotation motion coupled to the motion of the single (odd) nucleon within a reflection-asymmetric deformed potential with pairing correlations and fully microscopic treatment of the Coriolis interaction. The approach allows one to determine the energy and radiative decay properties of the ^{229m}Th isomer as a part of the entire low-lying positive- and negative-parity spectrum and transition probabilities observed in the nucleus ^{229}Th. On this basis, we have shown that the extremely small isomer energy can be explained as the consequence of a very fine interplay between the rotation-vibration degrees of freedom and the motion of the unpaired neutron. The model calculations predict for the reduced probability $B(M1)$ for magnetic decay of the isomer a value between 0.006 and 0.008 W.u. which is considerably smaller than earlier deduced values of 0.048 W.u. [16, 17] and 0.014 W.u. [18]. This result provides the currently adopted estimate for the ^{229m}Th nuclear life-time of about 10^4 sec explaining the experimental difficulties to observe the direct radiative decay of the isomer [19, 20] and suggests a new finer accuracy target for further measurements. In a subsequent work [21] we have calculated the magnetic moment of the isomer, $\mu_{\rm IS}$ and of the ground state (GS), $\mu_{\rm GS}$, by taking into account attenuation effects in the spin and collective gyromagnetic factors, without changing the model parameters originally adjusted in Ref. [15]. The result for $\mu_{\rm IS}$ in the range from $\mu_{\rm IS} = -0.25\mu_N$ to $-0.35\mu_N$ is in rather good agreement with the recent experimental values $-0.37(6)$

*e-mail: nminkov@inrne.bas.bg

[10] and (−0.3)–(−0.4) [11]. On the other hand, $\mu_{\rm GS}$ was obtained in the range $\mu_{\rm GS} = 0.53 - 0.66\ \mu_N$, overestimating the latest reported and older experimental values of 0.360(7) μ_N [22] and $\mu_{\rm GS} = 0.45\mu_N$ [23], respectively, and being in agreement with an earlier theoretical prediction $\mu_{\rm GS} = 0.54\mu_N$ based on the modified Woods-Saxon potential [24].

The aforementioned theoretical studies pointed out the complexity of the ^{229m}Th problem emphasizing on the need of consistent description of all related observables, detailed examination of the physical conditions for the forming of the isomer and further constraining of the arbitrariness in the model description to ensure maximal reliability of the obtained predictions as a tool in the establishing of the new nuclear clock standard. To this end in our very recent work [25] we investigated the shape deformation conditions under which such a low-energy isomer can appear in ^{229m}Th and examined the behaviour of the model solution in the relevant space of quadrupole and octupole deformations clarifying the limits of reliability of our model predictions. In this work we colligate the results of our approach obtained so far trying to outline the frames of the general prescription for the search and investigation of nuclear excitations on the border between nuclear and atomic physics.

In Sec. 2 we briefly present the model formalism. In Sec. 3 we give numerical results and illustrate the main points in the consistent study of ^{229m}Th shape characteristics and their influence on the isomer electromagnetic properties. In Sec. 4 concluding remarks are given.

2 The model approach

The model Hamiltonian is taken in the form [15]

$$H = H_{\rm s.p.} + H_{\rm pair} + H_{\rm qo} + H_{\rm Coriol}\,, \tag{1}$$

where $H_{\rm s.p.}$ is the s.p. Hamiltonian of Deformed Shell Model (DSM) with a Woods-Saxon (WS) potential including axial quadrupole (β_2) and octupole (β_3) deformation parameters [26], which provides the s.p. energies $E^K_{\rm sp}$ with given value of the projection K of the total and s.p. angular momentum operators $\hat{I}$ and $\hat{j}$, respectively on the intrinsic symmetry axis; $H_{\rm pair}$ is the standard Bardeen-Cooper-Schrieffer (BCS) pairing Hamiltonian [27]. This DSM+BCS part provides the quasi-particle (q.p.) spectrum $\epsilon^K_{\rm qp}$ as shown in Ref. [28]. $H_{\rm qo}$ represents oscillations of the even–even core with respect to quadrupole and octupole axial deformation variables mixed through a centrifugal (rotation-vibration) interaction [29, 30]; $H_{\rm Coriol}$ involves the Coriolis interaction between the even-even core and the unpaired nucleon (see Eq. (3) in [30]). It is treated as a perturbation with respect to the remaining part of (1) and then incorporated into the QO potential of $H_{\rm qo}$ defined for given angular momentum I, parity π and s.p. band-head projection K_b [15, 31].

The spectrum of Hamiltonian (1) is obtained in the form of coherent (with the same frequency) QO vibrations and rotations built on a q.p. state with $K = K_b$ and parity π^b [15, 31]

$$E^{\rm tot}_{nk}(I^\pi, K_b) = \epsilon^{K_b}_{\rm qp} + \hbar\omega\left[2n + 1 + \sqrt{k^2 + b\widetilde{X}(I^\pi, K_b)}\right], \tag{2}$$

where b is a model inertia parameter; $n = 0, 1, 2, ...$ and $k = 1, 2, 3, ...$ are radial and angular QO oscillation quantum numbers, respectively, with k odd (even) for the even (odd) parity states of the core [32]; ω is the frequency of the coherent QO mode (CQOM) [29, 30] and $\widetilde{X}(I^\pi, K_b)$ determines the centrifugal term in which the Coriolis mixing is taken into account [25]. The levels of the total QO core plus particle system, determined by a particular n and $k^{(+)}$ ($k^{(-)}$) for the states with given $I^{\pi=+}$ ($I^{\pi=-}$) form a split (quasi) parity doublet [33].

The Coriolis perturbed wave function corresponding to Hamiltonian (1) with the spectrum (2) is obtained in the form

$$\widetilde{\Psi}^{\pi,\pi^b}_{nkIMK_b} = \frac{1}{\widetilde{N}_{I\pi K_b}}\left[\Psi^{\pi,\pi^b}_{nkIMK_b} + A \sum_{\substack{\nu\neq b \\ (K_\nu = K_b \pm 1, \frac{1}{2})}} C^{I\pi}_{K_\nu K_b}\Psi^{\pi,\pi^b}_{nkIMK_\nu}\right], \tag{3}$$

in which the unperturbed core plus particle wave function $\Psi^{\pi,\pi^b}_{nkIMK_b}$ involving the projection K_b is mixed with the functions based on other s.p. states. In the case of non-zero octupole deformation $\beta = 0$ in the WS potential the s.p. states are characterized by average (mixed) parity and the corresponding s.p. wave functions are taken projected on the experimentally determined band-head parity π^b (for details see Eqs. (20)–(23) in [25]).

Having the wave function (3) we obtain the reduced $B(E1)$, $B(E2)$, $B(E3)$ and $B(M1)$ transition probabilities for the energy spectrum (2) [15] as well as the magnetic moments in the ground and isomeric states, $\mu_{\rm GS}$ and $\mu_{\rm IS}$, respectively [21] (for details see Ref. [25]). Because of the Coriolis mixing the states with different K_b values appear connected through electromagnetic transitions which otherwise would be suppressed due to the axial symmetry of the system. This determines the model mechanism allowing for the M1 and E2 radiative decay of the $K^\pi = 3/2^+$ IS to the $K^\pi = 5/2^+$ GS.

3 Transition rates and magnetic moments in ^{229}Th

In Ref. [15] we applied the above DSM-CQOM approach to the low-lying part of the experimental ^{229}Th spectrum [34], as shown in Fig. 1 of [15]. The theoretical spectrum was obtained in the form of an yrast quasi parity-doublet (QPD) built on the 5/2[633] ground-state s.p. orbital and non-yrast QPD built on the 3/2[631] orbital corresponding to the $3/2^+$ isomeric state. The model parameters, β_2 and β_3 entering DSM, the BCS pairing parameters, the collective CQOM parameters and the Coriolis mixing strength were determined so that both states $5/2^+$ GS and the isomeric $3/2^+$ were obtained as a quasi-degenerate pair, showing that the latter can be easily set in the range

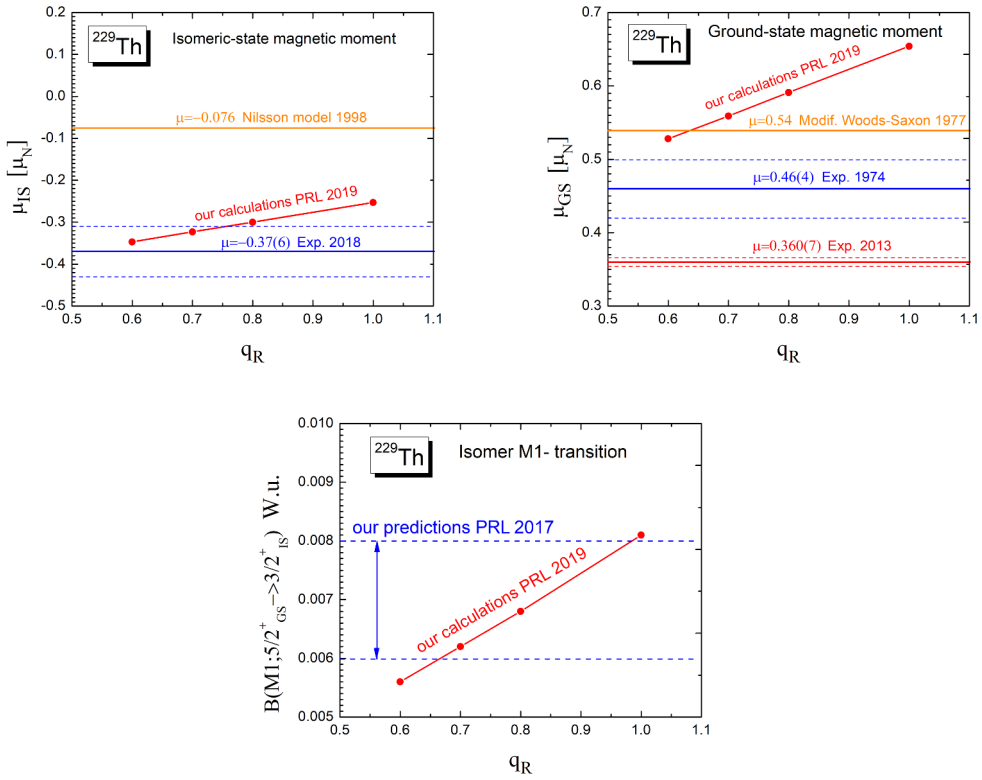

Figure 1. The calculated IS and GS magnetic moments and the isomer B(M1) decay rate in dependence on the quenching factor q_R. The dashed lines mark the experimental error bars for the magnetic moments and theoretical-prediction limits for B(M1). See the text for explanations.

of the experimental one through a very fine tuning of parameters with the excited QPD levels and the available experimental B(E2) and B(M1) values [35] being reproduced reasonably well. On this basis we have made predictions for the M1 and E2 decay probabilities for the $3/2^+$ isomer state given in Table I of [15].

In Ref. [21] we calculated the magnetic moments $\mu_{\rm GS}$ and $\mu_{\rm IS}$ of ^{229}Th corresponding to the parameters of the model description in [15] without further adjustment by only taking the commonly used quenching $q_s = 0.6$ of the spin gyromagnetic factor g_s and by considering several values for the quenching $q_R = 1, 0.8, 0.7, 0.6$ of the collective gyromagnetic factor g_R based on earlier studies of ^{229}Th [36, 37]. Here we illustrate this result in Fig. 1. We see that for $\mu_{\rm IS}$ (upper left plot) the theoretical predictions well approach the experimental value of $-0.37(6)\,\mu_N$ [10] firmly staying inside the uncertainty bars for $q_R = 0.7$ and 0.6. For $\mu_{\rm GS}$ we see (upper right plot) that although the theoretical values obtained with decreasing q_R approach the experimental values $0.360(7)\,\mu_N$ [22] and $\mu_{\rm GS} = 0.45\mu_N$ [23] they still remain outside of the uncertainty bars. At the same time the lower plot of Fig. 1 illustrates that the isomer B(M1) transition rate decreases with q_R. All these results show that more detailed consideration of the magnetic moments together with other observables in ^{229}Th needs to be done in order to assess the limits of reliability of our approach in determining the electromagnetic properties of the 8 eV isomer.

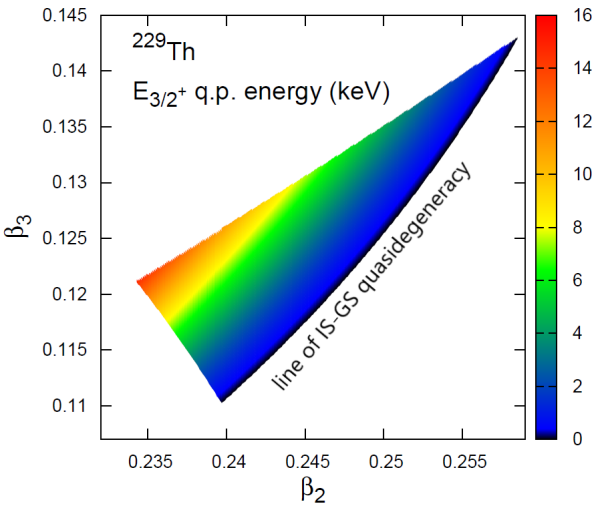

Figure 2. Q.p. energy (in keV) of the $3/2^+$ isomer orbital with respect to the $5/2^+$ GS orbital appearing in DSM within the model-defined space of QO deformations.

Thus, in Ref. [25] we implemented such a complex study of the deformation and electromagnetic properties of the ^{229m}Th isomer. First we implemented DSM calculations over a net in the β_2 and β_3 deformation space outlining the region where the GS and IS s.p. orbitals appear

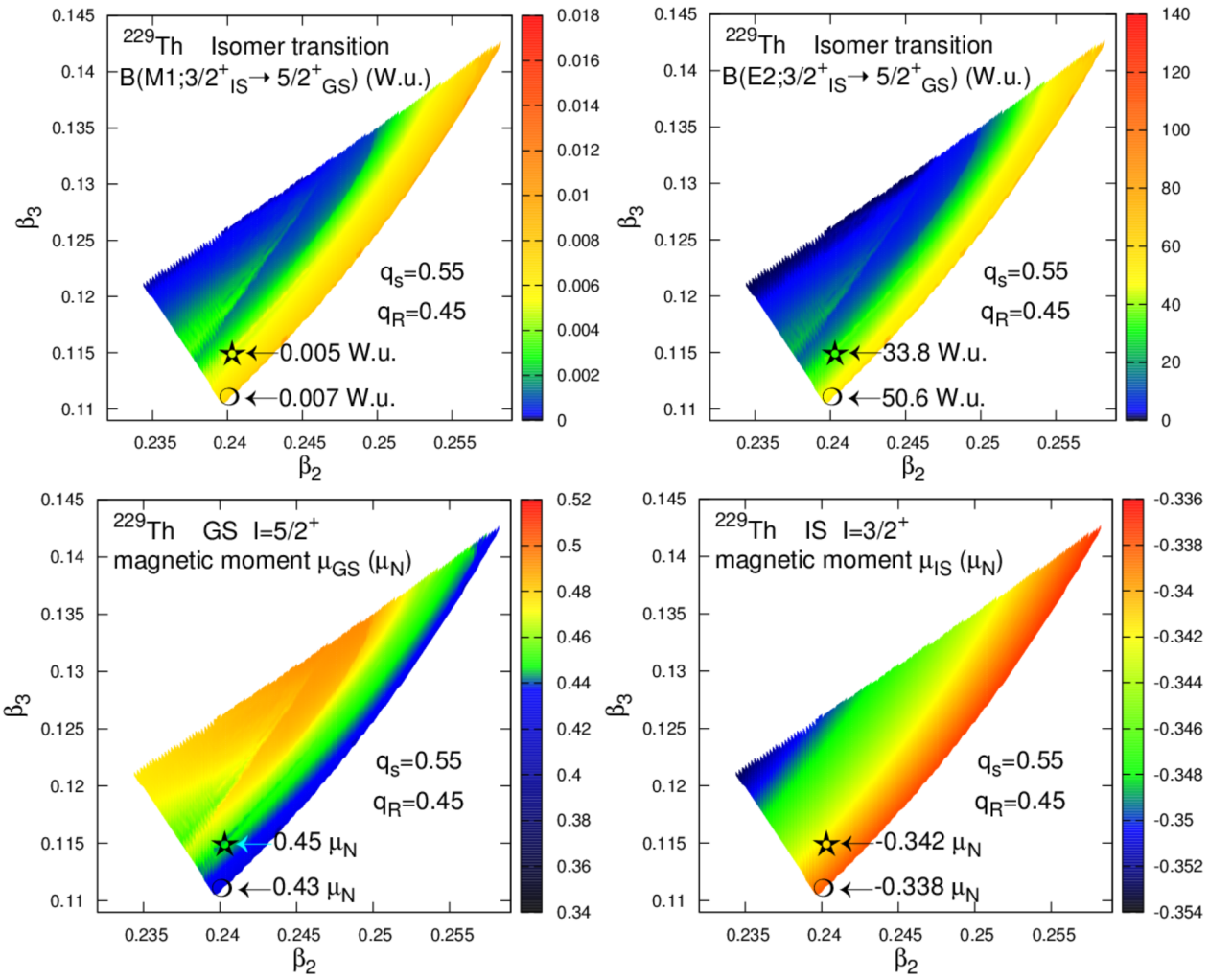

Figure 3. B($M1$), B($E2$) isomer transition rates and $\mu_{\rm GS}$ and $\mu_{\rm IS}$ values obtained by the model fits on a grid within the model-defined QO deformation space at $q_s = 0.55$ and $q_R = 0.45$. The open star indicates the location of the deformations (β_2,β_3)=(0.240, 0.115) adopted in Ref. [15]. The circle indicates the set (β_2,β_3)=(0.240, 0.111) situated closer to the degeneracy line. Adapted from [25].

with the correct K values and average parity. This region is illustrated in Fig. 2 where the q.p. energy corresponding to the $3/2^+$ isomer orbital with respect to the $5/2^+$ GS orbital is given as a function of β_2 and β_3. We can point out two important observations: i) the QO region allowing the correct orbitals configuration essentially includes non-zero octupole deformation; ii) there is a well determined line of IS-GS orbital degeneracy along which one may expect the isomer formation. This result already reveals the crucial role of the deformation for the appearance and the overall properties of the $3/2^+$ isomer. Then, as a second step, we performed massive model DSM-CQOM fits at each point in the deformation grid considering energies, transition rates and magnetic moments all together. This allowed us to examine the behaviour of the obtained model description for all observables of interest within the QO deformation space. In Fig. 3 we illustrate the result obtained for the isomeric B(M1) and B(E2) transition rates and the magnetic moments $\mu_{\rm GS}$ and $\mu_{\rm IS}$ with the quenching factors $q_s = 0.55$ and $q_R = 0.45$. We see that all these quantities exhibit a smooth behaviour in dependence on β_2 and β_3 with the physically interesting theoretical values appearing towards the IS-GS degeneracy line. We also remark that towards this line the model fairly well approaches the experimental isomer energy of about 8 eV. Considering the magnetic moments, now we find a region where $\mu_{\rm GS}$ (lower left plot) already reaches one of the experimental values $\mu_{\rm GS} = 0.45\mu_N$ [23], while for $\mu_{\rm IS}$ (lower right plot) the theoretical predictions always appear close to the experimental value of $-0.37(6)\ \mu_N$ [10]. Also, we see from the upper plots that the behaviour of the isomer transition rates within the QO space suggests a bit smaller values for the B(M1) and somehow larger values for the B(E2) transition compared to those predicted in Ref. [15].

4 Conclusion

Our study and all results presented in this work lead us to the important conclusion that the electromagnetic properties and subsequently the decay and life-time characteristics of the ^{229m}Th isomer are essentially determined by the collective and intrinsic (s.p.) manifestation of nuclear shape deformation. Therefore, its detailed analysis in the aspect of any model description aiming to reach precise

determination of the isomer energy and decay properties appears to be of a crucial importance. In a more general aspect the study suggests that the same dynamical mechanism may govern also in other nuclei excitations close to the border of atomic physics energy scale, thus paving the way for the systematic search for similar low-energy isomers in adjacent and remote nuclear regions.

5 Acknowledgments

This work is supported by the Bulgarian National Science Fund (BNSF) under Contract No. KP-06-N48/1. AP gratefully acknowledges funding by the Heisenberg Program of the Deutsche Forschungsgemeinschaft (DFG). The authors also acknowledge the support by Google Inc.

References

[1] B. R. Beck et al., Phys. Rev. Lett. **98**, 142501 (2007); LLNL-PROC-415170 (2009)
[2] C. J. Campbell et al., Phys. Rev. Lett. **108**, 120802 (2012)
[3] E. Peik and C. Tamm, Europhys. Lett. **61**, 181 (2003)
[4] E. Peik and M. Okhapkin, C. R. Phys. **16**, 516 (2015)
[5] E. V. Tkalya, Phys. Rev. Lett. **106**, 162501 (2011)
[6] T. Bürvenich et al., Phys. Rev. Lett. **96**, 142501 (2006)
[7] V. V. Flambaum, Phys. Rev. Lett. **97**, 092502 (2006)
[8] L. von der Wense et al., Nature (London) **533**, 47 (2016)
[9] B. Seiferle, L. von der Wense and P. G. Thirolf, Phys. Rev. Lett. **118**, 042501 (2017)
[10] J. Thielking, M. V. Okhapkin, P. Glowacki, D. M. Meier, L. von der Wense, B. Seiferle, C. E. Düllmann, P. G. Thirolf and E. Peik, Nature (London) **556**, 321 (2018)
[11] R. Müller et al., Phys. Rev. A **98**, 020503(R) (2018)
[12] B. Seiferle et al., Nature (London) **573**, 243 (2019)
[13] A. Yamaguchi et al., Phys. Rev. Lett. **123**, 222501 (2019)
[14] T. Sikorsky et al., Phys. Rev. Lett. **125**, 142503 (2020)
[15] N. Minkov and A. Pálffy, Phys. Rev. Lett. **118**, 212501 (2017)
[16] A. M. Dykhne and E. V. Tkalya, JETP Lett. **67**, 251 (1998)
[17] E. V. Tkalya, C. Schneider, J. Jeet and E. R. Hudson, Phys. Rev. C **92**, 054324 (2015)
[18] E. Ruchowska et al., Phys. Rev. C **73**, 044326 (2006)
[19] J. Jeet et al., Phys. Rev. Lett. **114**, 253001 (2015)
[20] A. Yamaguchi et al., New J. Phys. **17**, 053053 (2015)
[21] N. Minkov and A. Pálffy, Phys. Rev. Lett. **122**, 162502 (2019)
[22] M. S. Safronova, U. I. Safronova, A. G. Radnaev, C. J. Campbell and A. Kuzmich, Phys. Rev. A **88**, 060501(R) (2013)
[23] S. Gerstenkorn et al., J. Phys. (Paris) **35**, 483 (1974)
[24] R. R. Chasman, I. Ahmad, A. M. Friedman and J. R. Erskine, Rev. Mod. Phys. **49**, 833 (1977)
[25] N. Minkov and A. Pálffy, Phys. Rev. C **103**, 014313 (2021)
[26] S. Cwiok, J. Dudek, W. Nazarewicz, J. Skalski and T. Werner, Comp. Phys. Comm. **46**, 379 (1987)
[27] P. Ring and P. Schuck, *The Nuclear Many-Body Problem*, (Springer, Heidelberg, 1980)
[28] P. M. Walker and N. Minkov, Phys. Lett. B **694**, 119 (2010)
[29] N. Minkov, P. Yotov, S. Drenska, W. Scheid, D. Bonatsos, D. Lenis and D. Petrellis, Phys. Rev. C **73**, 044315 (2006)
[30] N. Minkov, S. Drenska, P. Yotov, S. Lalkovski, D. Bonatsos and W. Scheid, Phys. Rev. C **76**, 034324 (2007)
[31] N. Minkov, Physica Scripta **T154**, 014017 (2013)
[32] N. Minkov, S. Drenska, M. Strecker, W. Scheid and H. Lenske, Phys. Rev. C **85**, 034306 (2012)
[33] N. Minkov, S. Drenska, K. Drumev, M. Strecker, H. Lenske and W. Scheid, Phys. Rev. C **88**, 064310 (2013)
[34] http://www.nndc.bnl.gov/ensdf/
[35] http://www.nndc.bnl.gov/nudat2/indx_adopted.jsp
[36] S. G. Nilsson and O. Prior, Kgl. Dan. Vidensk. Selsk. Mat.-Fys. Medd. **32**, No. 16 (1961)
[37] H. Ton, S. Roodbergen, J. Brasz, and J. Blok, Nucl. Phys. A **155**, 245 (1970)